Hindawi
Advances in Materials Science and Engineering
Volume 2018, Article ID 3283907, 11 pages
https://doi.org/10.1155/2018/3283907

Research Article

Experimental Study on Physicochemical and Mechanical Properties of Mortar Subjected to Acid Corrosion

Runke Huo,[1] **Shuguang Li**,[1] **and Yu Ding**[2]

[1]*School of Civil Engineering, Xi'an University of Architecture and Technology, Xi'an 710055, China*
[2]*School of Civil and Resource Engineering, University of Science and Technology Beijing, Beijing 100083, China*

Correspondence should be addressed to Shuguang Li; lssgg2015@163.com

Received 25 January 2018; Revised 8 March 2018; Accepted 13 May 2018; Published 20 June 2018

Academic Editor: Giorgio Pia

The 28 days cured cement mortar samples were soaked in HCl (pH = 1 and 2) and H_2O (pH = 7) solutions for 90 days. By monitoring the ion concentration of H^+ and Ca^{2+} and measuring the changes in weight loss, longitudinal wave velocity, and uniaxial compressive strength values of the corroded mortar, the physicochemical and mechanical properties of the mortar specimens were studied. Experimental results indicate that the process of the mortar sample subjected to HCL erosion has apparent stage characteristics. In the initial stage of corrosion, the chemical reaction increased the porosity of the specimen, which leads to the decrease of longitudinal wave velocity of the samples. At the same time, the corrosion solution continuously penetrates into the mortar pore system, which leads to the increase of the mass, and it is considered that the diffusion process plays a leading role during this period. Moreover, the colloidal compounds generated by the chemical reaction can not only fill the pore space but also block the continuous reaction, which led to the increase of the longitudinal wave velocity of the specimen. With the prolonging of corrosion time and infiltration path, the pH value and the concentration of Ca^{2+} tend to be stable, the diffusion action is weakened, and the chemical reaction is continuous, which led to the decrease of the mass and wave velocity gradually. It is considered that the chemical reaction plays a leading role in this process. Based on the induction and analysis of the test results, a generalized porosity model regarding the increase of the porosity and the decrease of effective bearing area of the mortar sample was proposed. The relation between the uniaxial compressive strength and the corrosion time of the corroded mortar is deduced, and the unknown parameters are determined based on the regression analysis of the test data.

1. Introduction

Currently, chemical attacks are widely known as one of the most significant issues concerning the construction industry. The ACI committee (2001) reported several types of chemical attacks such as acid attacks, alkali attacks, chloride ingress, carbonation, and sulfate attacks [1]. All of these chemical attacks deteriorate the overall properties of cementitious materials [2–4]. The extensive acid medium makes concrete susceptible to acid attacks. Usually, the contaminated groundwater and industrial wastewater were considered to be the main reasons for deteriorating concrete's life. However, natural environments may also cause acid attacks on concrete structures. Acid attacks possess serious damage to the concrete structures. Many structures lose their serviceability every year due to the acidic environments [5–9]. This has led researchers to explore the deterioration properties of the acid solution of the concrete structure to find out an effective way to protect them [10]. Brown and Clifton [11] studied the mechanism of deterioration in cement-based materials and lime mortar. Sersale et al. [12] indicated that acid precipitation with a pH level ranging between 3.0 and 5.0 would affect cement and concrete. After that, a lot of literature focused on the different aspects of acid corrosion mortar matrix materials. Hu et al. [13] analyzed the change of chemical compositions and mineral compositions in hydrated cement paste which mixed with slag, fly ash, and SBR under the simulated acid rain condition. The results indicate that the acid rain attacking is an unceasing dissolution process of hydrating products such as $Ca(OH)_2$, C-S-H gel, hydrated calcium aluminate, and hydrated calcium ferrite gel. Fan et al.

Table 1: The chemical compositions of cement (%).

Sample	SiO_2	Al_2O_3	CaO	Fe_2O_3	MgO	SO_3	K_2O	Na_2O	Loss of ignition
Cement	19.58	7.12	63.48	3.22	2.64	2.33	0.49	0.23	2.97

[14] studied the material property of concrete under acid rain environment quantitatively. Results of concrete corrosion depth, mass loss, compressive strength, and elastic modulus were statistically analyzed and modeled. Yang et al. [15] studied the change of mortar properties in the strong acid environment. The study showed that weight loss could not accurately reflect the performance change of mortar in an acid environment, and multiple indexes are needed. Franzoni and Sassoni [16] investigated the correlation between stone microstructural characteristics and material degradation (regarding weight loss) in given environmental conditions. Song and Zhang [17] proposed a theoretical reaction rate model based on concentration boundary layer theory, and the applicability of the model was verified by the experimental data. Fan and Luan [18] indicated that the pore structure has a significant effect on the mechanical response and durability of concrete. The variation law of acoustic characteristics of sandstone in acid solution was studied by Huo et al. [19]. Experimental results showed that the acid corrosion rate of sandstone presented a certain stage characteristics. Xie et al. [20], Li et al. [21], Wei [22], and Chen et al. [23] studied the corrosion resistance of different types of cement mortar and their corrosion mechanism comprehensively. It has been found that deterioration of cementitious material specimens under acid rain attack was mainly caused by the coupling of H^+ and SO_4^{2-}, which led to higher porosity, and weight and strength loss of cementitious materials.

Reviewing the literature, it is apparent that the acid solution has an evident influence on cementitious materials. However, most of the current research is based on the sulfuric acid-based acid solution on the corrosion of concrete materials. Actually, hydrochloric acid corrosion of mortar materials is also an integral part of the study [24, 25]. Against this background, in this paper, the physical (mass and wave velocity), chemical (ion concentration), and mechanical properties of the Ordinary Type II Portland cement which is corroded by different pH values (pH = 1 and 2) of hydrochloric acid solution, distilled water solution (pH = 7) as a reference, are systematically studied. The corrosion process of mortar attacked by hydrochloric acid was explored. The mechanism of mortar attacked by hydrochloric acid was discussed. The relationship between compressive strength and time was deduced based on the generalized porosity model. Regression analysis indicates that the strength formula based on the model addressed in this study has high prediction accuracy.

2. Experimental Program

2.1. Materials. Ordinary Type II Portland cement complying with GB175-2007 [26] was used as the primary cementing material in this study. Tables 1 and 2 summarize the main features. The natural river sand obtained from Xi'an Chang River, China, was used as fine aggregate. The river sand fine aggregate has a particle size of less than 2.5 mm. The particle size distribution of river sand fine aggregate is shown in Table 3.

Table 2: The physical properties of cement.

Sample	Specific gravity (g/cm^3)	Blaine fineness (cm^2/g)	Compressive strength (MPa)	
			3 d	28 d
Cement	3.06	3489	17.58	43.65

The acidic environment was simulated by using hydrochloric acid (pH = 1 and 2) and the distilled water (pH = 7) as a reference.

2.2. Fabrication of Mortar Samples. Ninety cubic mortar samples ($70.7 \times 70.7 \times 70.7\ mm^3$) were made at a water/cement material mass ratio (w/c) of 0.485 with a sand-to-cement ratio (s/c) of 3.0. Table 4 summarizes the range of density, longitudinal wave velocity, and porosity of samples. All samples were processed similarly according to JGJ/T 98-2011 [27] standards. The mortars were cast into molds and kept in plastic sheeting for 24 h to avoid the evaporation of water. After removing the specimens from the molds, they were cured in a curing room for 28 days at a temperature of $20 \pm 2^{\circ}C$ and relative humidity not less than 95%. Then, mortar specimens were naturally dried in a cool dark place for several days.

2.3. Test Methods. Before soaking in the solutions, the specimens were dried in an electric oven at $105^{\circ}C$ for 24 h, and then, the initial dry weight, longitudinal wave velocity, and compressive strength were recorded. After that, the specimens were soaked in groups in HCl (pH = 1 and 2) and H_2O (pH = 7) solutions. There were three samples in each group. Reagent bottle with a volume of 10 L was used to avoid evaporation. The solution was renewed every ten days. The wet weight and longitudinal wave velocity of each sample were measured every ten days. The ion concentration of H^+ and Ca^{2+} of the acidic media was monitored every 3, 7, and 10 days. Uniaxial compression strength following GB/T17671-1999 [28] of the specimens after being subjected to acid attack was tested at 10, 20, 30, 40, 50, 60, 70, 80, and 90 days. Before the compression strength test, all the specimens were cured in the curing room at a temperature of $20 \pm 2^{\circ}C$ and relative humidity not less than 95% for seven days. To get precise data, the tests results appeared in this paper are the average value of one group (three samples).

3. Results and Discussion

3.1. Analysis of Physical Properties of Mortar Subjected to Acid Corrosion. The physical properties of acid-corroded mortar are characterized by definition of mass change rate and wave velocity change rate.

Table 3: The particle size distribution of fine aggregate.

Sieve size (mm)	0.16	0.32	0.63	1.25	2.5
Cumulative pass amount (%)	0	5	35	75	100

Table 4: The physical properties of mortar.

Sample	Density (g/cm^3)	Wave velocity (m/s)	Porosity (%)
Mortar	2.04~2.12	3918~4159	13.52~14.16

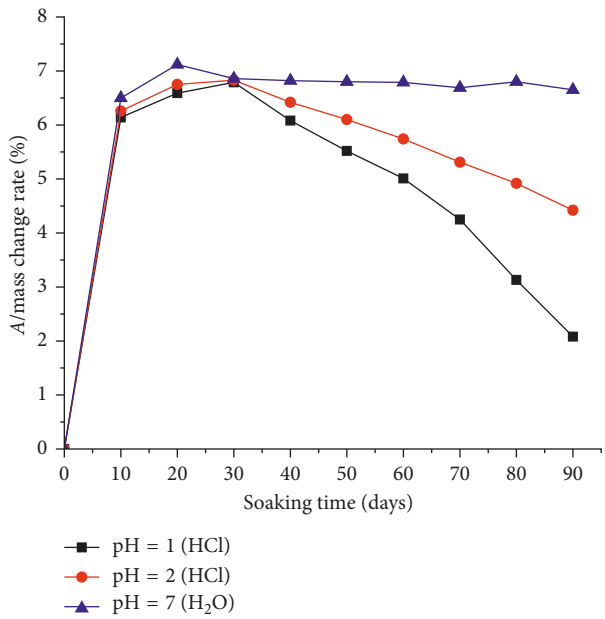

Figure 1: Mass change rate (%) of the mortar specimens in solutions with different pH values.

3.1.1. Mass Change Rate. The mass change rate of the acid-corroded mortar is defined as follows:

$$A = \frac{M_{it} - M_{i0}}{M_{i0}} \times 100\%, \quad (1)$$

where A is the mass change rate of the mortar and M_{i0} and M_{it} are the weight of the mortar before and after soaking in the acid solution, respectively.

The resulting mass change rate of mortar samples in different concentrations (pH value) of solutions is shown in Figure 1. It is observed in the figure that, in the first stage (0~10 days) of soaking, the mass change rate of the specimen in three solutions increased rapidly. When the immersion corrosion reached 20 days, the mass change rate of the sample in H_2O (distilled water) with pH = 7 reached the maximum value of 7.12% and then gradually stabilized. After 30 days of immersion corrosion, the mass change rate of the sample in HCl (hydrochloride) with pH = 1 and 2 reached the maximum value of 6.83% and 6.86%, respectively, and then decreased gradually. Moreover, it reduces faster in the solution of pH = 1 than that of pH = 2.

The results above demonstrate that the mass change rate of the mortar sample varies at different times in the solution with different pH values. Before the specimen reaches the maximum mass change rate, the dissolution of hydrochloric acid to mortar (chemical reaction) increases the connectivity of the porous system and the porosity of the sample, under the diffusion effect, and corrosion solution continues to penetrate into the porous spaces that were not accessible to water before acid attack, making the mass change rate of the mortar sample to increase. After the sample reaches the maximum mass change rate, it has sufficient time to react chemically with calcium hydroxide and calcium silicate hydrate in the mortar, which causes its weight to decrease gradually. Besides, the smaller the pH value (the stronger the acidity), the more the weight loss of the sample.

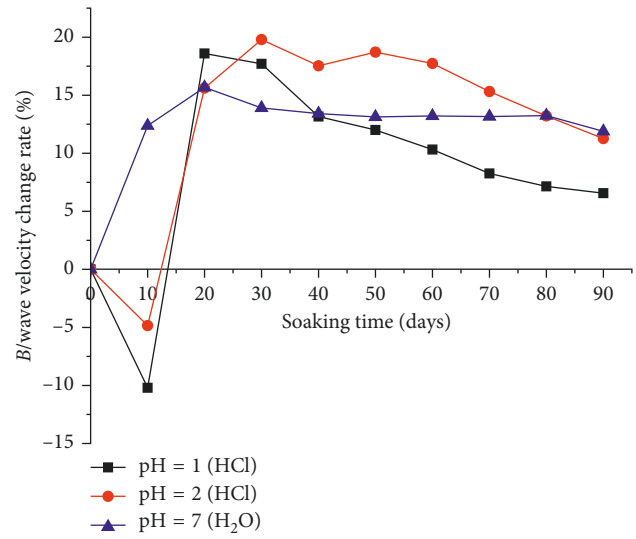

Figure 2: Wave velocity change rate (%) of the mortar specimens in solutions with different pH values.

3.1.2. Wave Velocity Change Rate. Wave velocity change rate of the acid-corroded mortar is defined as follows:

$$B = \frac{v_{it} - v_{i0}}{v_{i0}} \times 100\%, \quad (2)$$

where B is the wave velocity change rate of the mortar and v_{i0} and v_{it} are the wave velocity of the mortar before and after soaking in the acid solution, respectively.

Figure 2 shows the wave velocity change rate (%) of the mortar specimens in solutions with different pH values. It is observed in the figure that, in the first stage (0~10 days) of soaking in HCl solution with pH = 1, the reaction of the mortar specimen and acid solution increased the porosity of the specimen, and the chemical softening of the mortar skeleton resulted in the readjustment of the three-phase ratio of the solid, liquid, and gas phase, which reduced the longitudinal wave velocity of the mortar sample. The wave velocity change rate decreased to 10.2% after 10 days of corrosion. In the second stage (10~20 days) of immersion, with the extension of the corrosion time and the infiltration path, the cement paste was solubilised by the acid solution and fill porous spaces that previously contained air and were not accessible to water. Moreover, colloidal compounds (silica, aluminum hydroxide, iron hydroxide, etc.) with

strong adsorption capacity and compactness generated by the reaction blocked the contact between HCl solution and noncorroded mortar, the corrosion rate slowed down, and at the same time, the variation of the ratio of three-phase composition tends to improve. All this make the longitudinal wave velocity increase, and the wave velocity change rate increased to 18.6% on the 20th day. Then, the chemical reaction tends to stabilize, and the longitudinal wave velocity of the specimen decreases gradually.

The changed law of wave velocity change rate of the sample in the HCl solution with pH = 2 was similar to that in the HCl solution with pH = 1. The wave velocity change rate reduced in the first stage (0~10 days) and decreased to −10.20% on the 10th day and then, increased in the following two phases (10~20 and 20~30 days) with the maximum of 19.79% occurring on the 30th day, indicating that the chemical reaction rate slowed down in HCl solution with pH = 2 than that with pH = 1.

Compared with the HCl solution, the wave velocity change rate of mortar soaked in the distilled water (pH = 7) was also monitored; it was found from the figure that the wave velocity changes rate of the samples reached its maximum value of 15.68% on the 20th day, and then, its change is stable basically.

3.1.3. Discussion on the Mechanism of Wave Velocity Change of Acid-Corroded Mortar. Based on the Fermat Principle, Han et al. [29] established the relationship between the porosity and longitudinal wave velocity of saturated mortar and verified its applicability by experimental data. The relationship can be expressed as follows:

$$\frac{1}{v_p} = \frac{1-n_0}{v_m} + \frac{n_0}{v_f}, \tag{3}$$

where v_p is the measured longitudinal wave velocity of the saturated mortar, v_m is the longitudinal wave velocity of the mortar particle skeleton, v_f is the longitudinal wave velocity of the liquid in the mortar pores, and n_0 is the porosity of the mortar.

According to the above ideas, the present paper attempted to establish the relationship between longitudinal wave velocity and porosity of mortar subjected to acid corrosion. The following assumptions were made to simplify the analysis:

(1) The initial state of the mortar specimen is a two-phase medium composed of the solid matrix and porous, and the chemical corrosion does not make the mortar skeleton change in nature; that is, v_m (5300 m/s in this paper) is unchanged before and after corrosion.

(2) It is considered that the volume of pores formed in the mortar after acid corrosion is wholly filled with acid solution, and the density of the acid solution is approximately equal to the density of water; that is, v_f (1500 m/s in this paper) is unchanged.

(3) The acid-corroded mortar can be simplified as the corrosive zone and the noncorrosive zone, and the volume of the corrosive zone includes the volume of the pores increased by the chemical reaction. Also, it is affected by the decrease of pore volume due to the blocking effect of the colloidal compounds generated by the chemical reaction.

(4) It is considered that, before the corrosion time of T, the reaction rate of mortar and hydrochloric acid is faster than that of formation of colloidal compounds, and during this period, the porosity of the mortar sample increases, which makes $n_a > n_0$. After the corrosion time of T, the chemical reaction rate slows down, the formation rate of colloidal compounds accelerates, and the colloidal compounds produced by the chemical reaction will hinder the reaction between mortar and hydrochloric acid, and during this period, the porosity of the specimen decreases, which makes $n_a < n_0$.

According to (3) and the above assumptions, the relationship between the porosity and the longitudinal wave velocity of the acid corrosion mortar can be deduced as follows:

$$\frac{1}{v_p^1} = \frac{1-n_a}{v_m} + \frac{n_a}{v_f}, \tag{4}$$

where v_p^1 is the measured longitudinal wave velocity of the mortar after acid corrosion, v_m is the longitudinal wave velocity of the mortar particle skeleton, v_f is the longitudinal wave velocity of the acid solution, and n_a is the porosity of the mortar after soaking T days.

Equation (3) minus (4) gets the following formula:

$$\frac{1}{v_p} - \frac{1}{v_p^1} = \frac{1-n_0}{v_m} + \frac{n_0}{v_f} - \left(\frac{1-n_a}{v_m} + \frac{n_a}{v_f}\right) = (n_a - n_0)\left(\frac{1}{v_m} - \frac{1}{v_f}\right). \tag{5}$$

Due to $v_m > v_f$, the following equation can be obtained from formula (5) when $n_a > n_0$:

$$\frac{1}{v_p} - \frac{1}{v_p^1} < 0, \text{ namely, } v_p^1 < v_p. \tag{6}$$

The results of (6) are a reasonable explanation of the phenomenon that the wave velocity change rate is negative on the 10th day (Figure 2) and the wave velocity decreases in acid solution.

Due to $v_m > v_f$, the following equation can be obtained from formula (5) when $n_a < n_0$:

$$\frac{1}{v_p} - \frac{1}{v_p^1} > 0, \text{ namely, } v_p^1 > v_p. \tag{7}$$

The results of (7) is a reasonable explanation of the phenomenon that the wave velocity change rate is positive on the 20th, 30th, 40th, 50th, 60th, 70th, 80th, and 90th day (Figure 2) and the wave velocity increases in acid solution.

3.2. Analysis of Chemical Properties of Mortar Subjected to Acid Corrosion. The chemical properties of acid corrosion mortar are analyzed by monitoring the concentration of hydrogen ions (pH value) and calcium ions in the soaking solution.

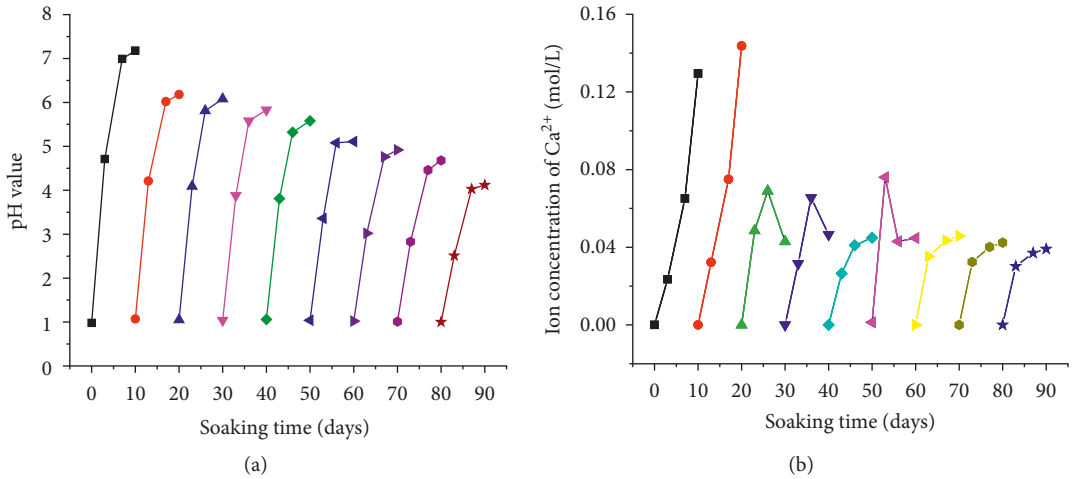

FIGURE 3: Concentration curves of (a) H^+ and (b) Ca^{2+} in HCl solution (pH = 1) at different periods.

Figures 3(a) and 3(b) show the concentration curves of H^+ and Ca^{2+} in HCl solution (pH = 1) at each stage (10 days), respectively. As observed in the Figure 3(a), in each stage (10 days), the pH value of the solution increases with the extension of immersion time. Within 0~10 days, the pH values of the solution were 2.7, 6.9, and 7.2 at day 3, 7, and 10, respectively. The solution was neutral after day 7. Within 10~20 days, the change law of the pH value is basically the same as that of 0~10 days. However, the solution showed weak acidity on day 20. With the extension of soaking time, the acidity of the solution became stronger after the end of each stage (pH = 6.2, 6.0, 5.8, 5.5, 5.1, 4.9, and 4.6 and 4.1 at day 20, 30, 40, 50, 60, 70, 80, and 90). Figure 3(b) shows that the concentration of Ca^{2+} increased gradually within 0~20 days, which is 0.1295 and 0.1437 mol/L at day 10 and 20, respectively. Then, the concentration of Ca^{2+} is about 0.045 mol/L after the end of each stage.

Figures 4(a) and 4(b) show the concentration curves of H^+ and Ca^{2+} in HCl solution (pH = 2) at each stage (10 days), respectively. It can be seen from Figure 4(a) that the solution became alkaline at day 3, which demonstrates the solubility of the colloidal compounds produced by the reaction is decreased, and that it is conducive to the formation of the colloid compounds. Figure 4(b) shows that the dissolution of Ca^{2+} in HCl solution with pH = 2 at each stage (10 days) is basically the same as that of pH = 1.

The concentration curves of H^+ and Ca^{2+} in H_2O solution (pH = 7) at different periods are shown in Figures 5(a) and 5(b) compared to HCl solution. The changed law of the pH value and the concentration of Ca^{2+} is basically the same as that of HCl solution. The solution became alkaline at day 3 (Figure 5(a)), and the pH is between 10 and 12, which demonstrates that the mortar itself is alkaline. The maximum value of Ca^{2+} appeared in 20~30 days, and then, it stabled at about 0.00001 mol/L.

3.3. Discussion on the Mechanism of Mortar Attacked by Hydrochloric Acid. The main chemical equation for the reaction of hydrochloric acid with mortar is as follows:

$$\begin{aligned} Ca(OH)_2 + 2HCl &\longrightarrow CaCl_2 + 2H_2O \\ xCaO \cdot ySiO_2 \cdot nH_2O + 2xHCl &\longrightarrow xCa^{2+} + 2xCl^- \\ &\quad + ySi(OH)_4 \\ &\quad + (x + n - 2y)H_2O \end{aligned} \tag{8}$$

As can be seen from the above reaction formula, due to the strong acid effect of HCl solution, a large number of calcium hydroxide is neutralized and produced a mass of calcium chloride with high solubility, resulting in the decomposition of hydrated calcium silicate in the mortar samples. Hydrochloric acid, on the contrary, reacts directly with hydrated calcium silicate. In this way, the gel of the mortar pore structure is considerably damaged, causing the increase of porosity and the decrease of effective bearing area of mortar samples, resulting in the deterioration of the physical and mechanical properties of the mortar samples.

Through the observation of the experiment and the analysis of the test results, it is known that the interaction between hydrochloric acid and mortar can be regarded as a physicochemical process of multiphase. The process can be divided into three stages from the outside to the inside for the mortar sample subjected to hydrochloric acid corrosion [30, 31]:

(1) The acidic medium diffuses into the pores or capillaries of the mortar. If the chemical reaction occurs faster in the wet film on the porous mortar surface, the medium is completely absorbed and does not penetrate into the inside of the mortar sample until the sample absorbs medium and is saturated, resulting in a significant increase of the porosity of the corroded area of the specimen. In this case, the process of the mortar being corroded by hydrochloric acid can be regarded as controlled by the diffusion effect.

(2) The acidic medium reacts with the various mineral compositions that make up the mortar. If the rate of

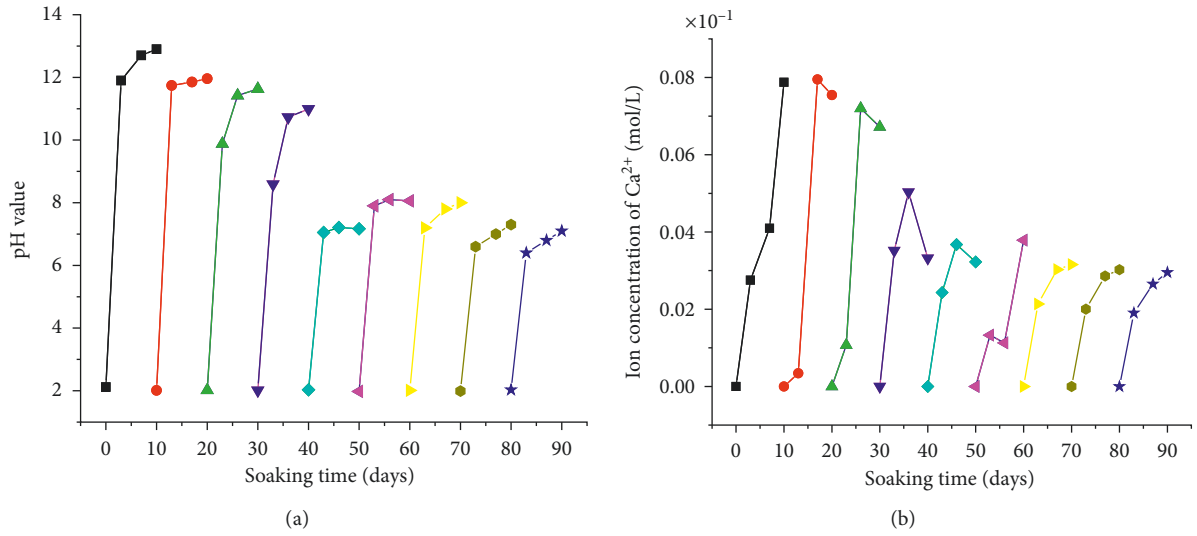

Figure 4: Concentration curves of (a) H^+ and (b) Ca^{2+} in HCl solution (pH = 2) at different periods.

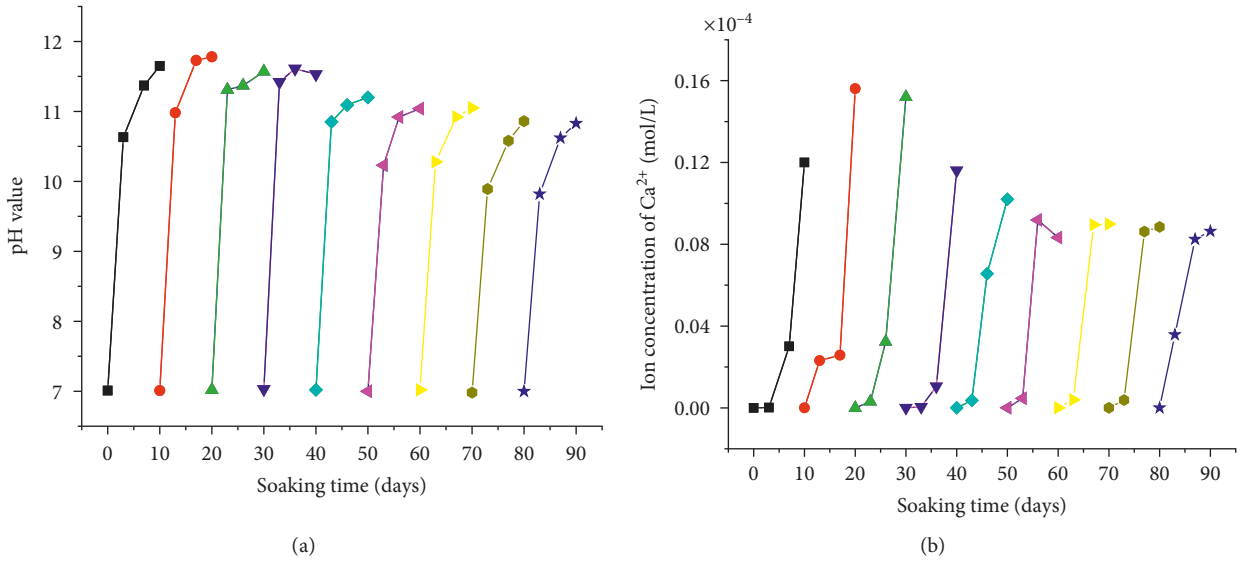

Figure 5: Concentration curves of (a) H^+ and (b) Ca^{2+} in H_2O solution (pH = 7) at different periods.

penetration of acidic media into the mortar is faster than the rate at which the acidic medium is absorbed by the mortar, then the acidic medium is not all consumed in the corroded zone, but to the internal of the sample to form a broader reaction zone. In this case, the process of the mortar being corroded by hydrochloric acid can be regarded as controlled by the chemical kinetics effect.

(3) With the increase of corrosion time, the reaction products are gradually precipitated or dissolved.

Therefore, under normal circumstances, it is considered that the acidic medium is completely absorbed and does not penetrate into the inside of the mortar sample in the initial stage of acid corrosion to mortar, and at this time, the reaction of mortar and hydrochloric acid is controlled by diffusion. With the prolongation of etching time, the immersion solution becomes saturated, and the acidic medium penetrates into the specimen to form a deeper reaction zone, at which time the corrosion process is controlled by chemical kinetics, and then, the reaction products are gradually precipitated or dissolved.

3.4. Analysis of Mechanical Properties of Mortar Subjected to Acid Corrosion. To study the deterioration degree of the mechanical properties of the mortar subjected to hydrochloric acid corrosion, the uniaxial compression test was carried out on the mortar subjected to corrosion solution with a different pH value. Based on the analysis of the increase of porosity and the decrease of effective bearing area of the mortar after hydrochloric acid corrosion, combined with uniaxial compression test results, a generalized porosity model of the compressive strength of the mortar corroded by hydrochloric

acid was established, and the relationship between the uniaxial compressive strength and corrosion time was deduced.

3.4.1. Compressive Strength Analysis. The uniaxial compressive strength of mortar immersed in different pH solutions for different time can be seen in Figure 6 and Table 5. As observed in Figure 6 and Table 5, the smaller the pH value of the acid solution, the greater the decrease of the compressive strength of mortar. After 90 days, the compressive strength of the mortar in pH = 1 HCl solution decreased from 43.56 to 20.05 MPa, decreased by 53.97%. The compressive strength of the mortar in pH = 2 HCl solution decreased from 44.21 to 28.56 MPa, decreased by 35.40%. Besides, the strength of the dry mortar changed greatly in day 0~30. It is reduced from 43.56 to 30.88 MPa (pH = 1 HCl) and 44.21 to 36.02 MPa (pH = 2 HCl), and the decrease range is 29.10% and 18.52%, respectively. The compressive strength change of mortar in pH = 7 H_2O solution is relatively stable, and it decreased from 43.28 to 40.08 MPa, decreased by 7.39%.

3.4.2. Relationship between Uniaxial Compressive Strength and Corrosion Time of Mortar. The pore is the main reason for the impact of mortar strength. To obtain the porosity generalization model for compressive strength of mortar subjected to acid corrosion, the following assumptions are made:

Take the differential unit body of mortar with unit thickness for example. The length, width, and depth of the differential element are all b, as shown in Figure 7(b). It is considered that the accumulated pore of a differential element of mortar produced by the chemical action can be obtained through the rotation of the cycloidal equation. The radius of the cycloid circle is a, as shown in Figure 7(a).

(1) Mortar sample is treated as two-phase media consisting of mortar matrix and pores.

(2) The compressive strength of the mortar specimen is inversely proportional to the area of acid corrosion.

(3) The increase of the pores and the decrease of the matrix bearing area of the specimen are mainly caused by chemical corrosion.

The cycloidal equation is shown as follows:

$$\begin{aligned} x &= a(\theta - \sin\theta), \\ y &= a(1 - \cos\theta), \end{aligned} \tag{9}$$

where θ is the rotation angle of the circle in the cycloid, as shown in Figure 7(a). Cycloid volume with the x-axis as the rotation axis can be written as follows:

$$v = 2\int_0^{\pi a} \pi y^2\,dx = 2\int_0^{\pi} \pi a^3 (1-\cos\theta)^3 d\theta = 5\pi^2 a^3. \tag{10}$$

In this case, the porosity of the differential element can be expressed as follows:

$$n_p = \frac{v}{b^3} = \frac{5\pi^2 a^3}{b^3}. \tag{11}$$

The area surrounded by the cycloid and the x-axis can be expressed by the following formula:

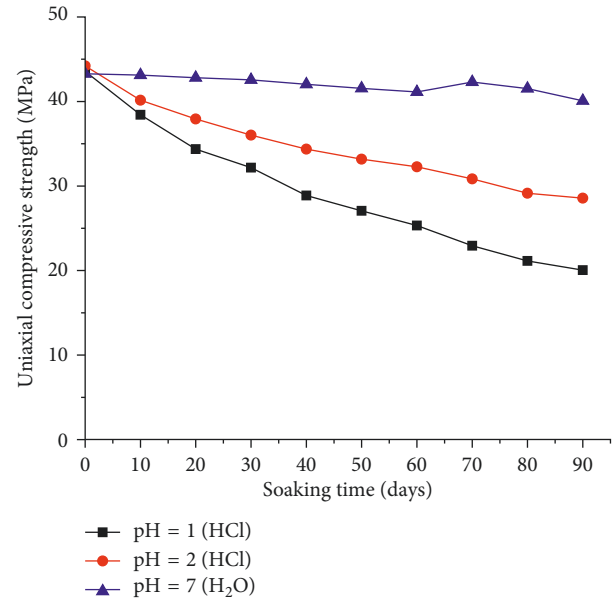

Figure 6: Uniaxial compressive strength of the mortar specimens in solutions with different pH values.

$$A = 2\int_0^{\pi a} y\,dx = 2\int_0^{\pi} a^2 (1-\cos\theta)^2 d\theta = 3\pi a^2. \tag{12}$$

Hence, the maximum area of the rotating cycloid can be given by the following formula:

$$A_{\max} = 2A = 6\pi a^2. \tag{13}$$

Because the compressive strength is proportional to the active bearing area of the sample, after soaking for t days, the compressive strength of the mortar unit can be expressed as follows:

$$\sigma_{ft} = \sigma_{f0}\left(b^2 - 6\pi a^2\right), \tag{14}$$

where σ_{ft} is the compressive strength after t days' corrosion and σ_{f0} is the initial compressive strength of the mortar unit.

The following equation can be obtained from formula (11) and (14):

$$\sigma_{ft} = \sigma_{f0}\left(b^2 - 1.40 b^2 n_p^{2/3}\right). \tag{15}$$

Set

$$\chi = \frac{\sigma_{ft}}{\sigma_{f0}}, \tag{16}$$

where χ is the compressive strength ratio.

Then, formula (15) can be expressed as follows:

$$\chi = b^2\left(1 - 1.40 n_p^{2/3}\right). \tag{17}$$

The process of acid corrosion of the mortar specimen is the diffusion process of the hydrogen ion in the sample, and the increase of corrosion depth is the main reason for the rise in porosity. Formula (17) gives the relationship between the compressive strength ratio of the mortar element and its porosity.

It is assumed that the porosity of the sample is proportional to the area of the mortar corroded by the acid

Table 5: Uniaxial compressive strength of mortar.

HCl (pH = 1)			HCl (pH = 2)			H_2O (pH = 7)		
T (days)	S	M (MPa)	T (days)	S	M (MPa)	T (days)	S	M (MPa)
0	#1~3	43.56	0	#31~33	44.21	0	#61~63	43.28
10	#4~6	38.42	10	#34~36	40.15	10	#64~66	43.12
20	#7~9	34.37	20	#37~39	37.93	20	#67~69	42.81
30	#10~12	30.88	30	#40~42	36.02	30	#70~72	42.56
40	#13~15	28.87	40	#43~45	34.36	40	#73~75	42.03
50	#16~18	27.06	50	#46~48	33.18	50	#76~78	41.56
60	#19~21	25.32	60	#49~51	32.27	60	#79~81	41.13
70	#22~24	22.93	70	#52~54	30.85	70	#82~84	42.31
80	#25~27	21.14	80	#55~57	29.14	80	#85~87	41.52
90	#28~30	20.05	90	#58~60	28.56	90	#88~90	40.08

S represents the serial number of the mortar specimen; M represents the mean value (three samples) of compressive strength.

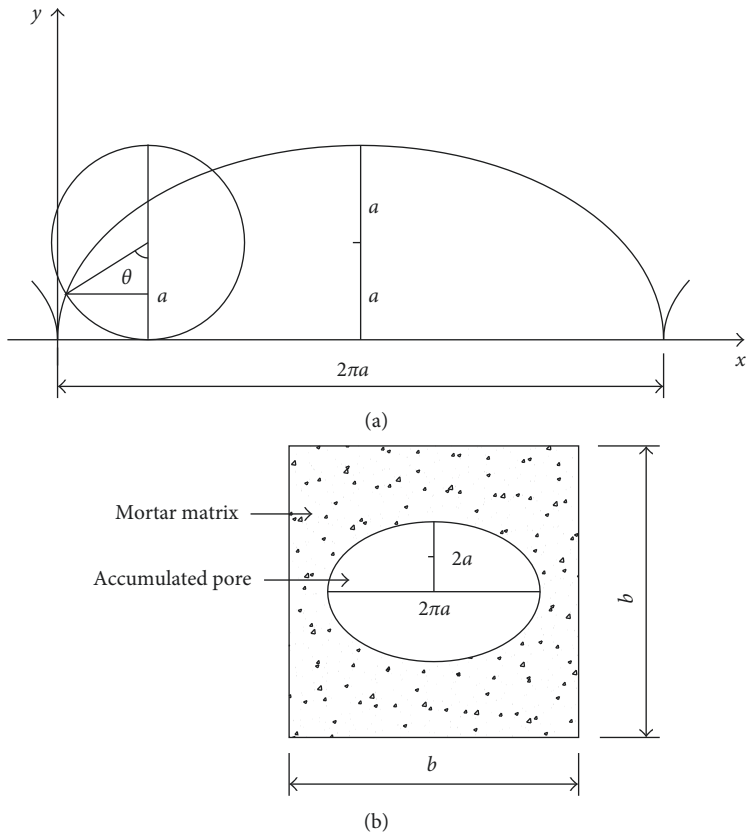

Figure 7: Sketch of a generalized model of the mortar sample. (a) Cycloid model. (b) Mortar unit body.

solution, as shown in Figure 8, the length of the cube sample is d, and the corrosion depth of the cube is $d(t)$. Then,

$$n_p \propto d^2 - [d - 2d(t)]^2, \tag{18}$$

which can also be written as follows:

$$n_p = \gamma\left\{d^2 - [d - 2d(t)]^2\right\} = 2\gamma\left[d(t) \cdot d - d^2(t)\right]. \tag{19}$$

Then, the following equation can be obtained from formula (17) and (19):

$$\chi = b^2 - 1.40b^2\left\{2\gamma\left[d(t) \cdot d - d^2(t)\right]\right\}^{2/3}. \tag{20}$$

Set

$$\left\{2\gamma\left[d(t) \cdot d - d^2(t)\right]\right\}^{2/3} = \lambda d^{2/3}(t) + \eta d^{4/3}(t). \tag{21}$$

where γ, λ, and η are all undetermined coefficients.

Then, χ can be expressed by formula (20) and (21):

$$\chi = b^2 - 1.40b^2\left[\lambda d^{2/3}(t) + \eta d^{4/3}(t)\right]. \tag{22}$$

Literature [32] and [33] obtained the damage depth formula of the one-dimensional acid corrosion through a large number of corrosion tests, which is given by

$$d(t) = a\sqrt{t}, \tag{23}$$

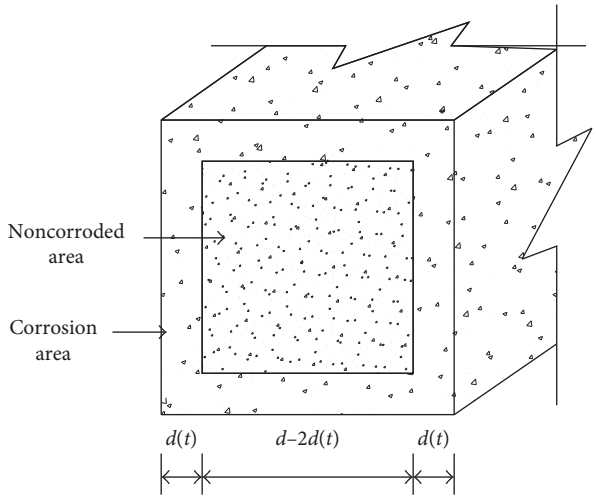

Figure 8: Corrosion depth of the mortar specimen.

where $d(t)$ is the corrosion depth, t is the soaking time (day or year), and a is a influenced coefficient, which is related to the type and concentration of acid and the composition of mortar sample.

The following equation can be obtained from formula (22) and (23):

$$\chi = \frac{\sigma_{ft}}{\sigma_{f0}} = a_1 + a_2 t^{1/3} + a_3 t^{2/3}. \quad (24)$$

where $a_i\,(i = 1, 2, 3)$ is the experimental constant.

Equation (24) expresses the relationship between uniaxial compressive strength and corrosion time of mortar under the action of the hydrochloric acid solution. $a_i\,(i = 1, 2, 3)$ can be fitted (Figures 9(a) and 9(b)) by a regression equation with the help of the data obtained from the experiment (Table 6).

Then, (24) can be expressed as follows:

For the hydrochloric acid solution of pH = 1,

$$\chi = \frac{\sigma_{ft}}{\sigma_{f0}} = 1.126 - 0.1t^{1/3} - 0.011t^{2/3}. \quad (25)$$

For the hydrochloric acid solution of pH = 2,

$$\chi = \frac{\sigma_{ft}}{\sigma_{f0}} = 1.024 - 0.026t^{1/3} + 0.013t^{2/3}. \quad (26)$$

The fitting curves demonstrate that the theoretical curves are generally in good agreement with the experimental results and the relationship between uniaxial compressive strength and corrosion time of mortar subjected to hydrochloric acid solution addressed in this study has high prediction accuracy.

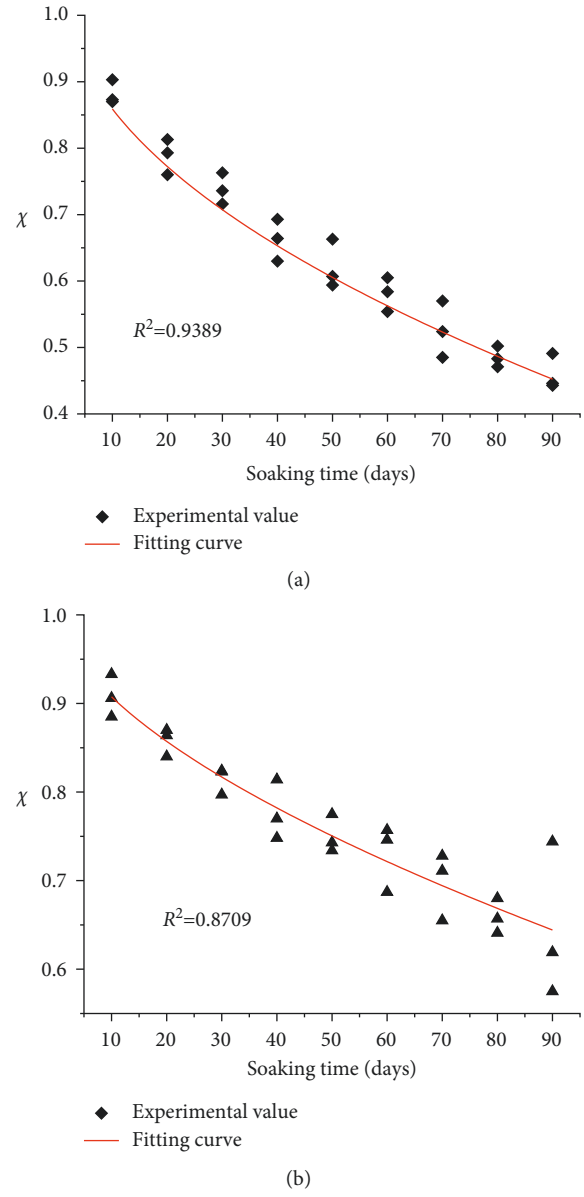

Figure 9: The relationship between the compressive strength ratio and soaking time of mortar attacked by HCl solution: (a) pH = 1; (b) pH = 2.

4. Conclusions

Based on the results of this study, the following conclusions can be drawn:

(1) The different stages of immersion corrosion were quantitatively described with the defined mass change rate and wave velocity change rate as well as the concentration changes of H^+ and Ca^{2+} in the immersion solution, which adequately reflected the process of the mortar sample being corroded by hydrochloric acid comprehensively. Moreover, the relationship between the porosity and the wave velocity of the mortar corroded by hydrochloric acid was tried to establish, by which the mechanism of wave velocity variation appeared in the experiment can be well explained.

(2) The mechanism of mortar attacked by hydrochloric acid was discussed. The analysis showed that the process of the mortar sample subjected to hydrochloric acid erosion had apparent stage characteristics. In the initial stage of immersion corrosion, the chemical reaction increased the pH value and the concentration of Ca^{2+}, and the porosity of the specimen also increases, which lead to the decrease of

Table 6: Uniaxial compressive strength ratio of mortar.

HCl (pH = 1)					HCl (pH = 2)				
T (days)	S		χ		T (days)	S		χ	
10	#4~6	0.903	0.873	0.870	10	#34~36	0.933	0.906	0.885
20	#7~9	0.760	0.813	0.793	20	#37~39	0.870	0.840	0.864
30	#10~12	0.736	0.763	0.716	30	#40~42	0.797	0.823	0.824
40	#13~15	0.630	0.664	0.693	40	#43~45	0.770	0.748	0.814
50	#16~18	0.607	0.594	0.663	50	#46~48	0.734	0.743	0.775
60	#19~21	0.554	0.584	0.605	60	#49~51	0.687	0.757	0.746
70	#22~24	0.485	0.524	0.570	70	#52~54	0.655	0.711	0.728
80	#25~27	0.483	0.502	0.471	80	#55~57	0.641	0.657	0.680
90	#28~30	0.446	0.491	0.443	90	#58~60	0.575	0.619	0.744

S represents the serial number of the mortar specimen; χ represents the strength ratio of mortar.

longitudinal wave velocity. Meanwhile, the corrosion solution continuously penetrates into the mortar pore system under the diffusion effect, which leads to the increase of weight of the specimen, and it is considered that the diffusion process plays a leading role during this period. The colloidal compounds generated by the reaction can not only fill the pore space but also block the continuous reaction to some extent, which leads to the increase of the longitudinal wave velocity of the specimen. With the prolonging of corrosion time and infiltration path, the pH value and the concentration of Ca^{2+} in soaking solution tend to be stable, the diffusion action is weakened, and the chemical reaction is continuous, which led to decrease of the weight and the wave velocity of the specimen gradually. It is considered that the chemical reaction plays a leading role in this process.

(3) Based on the induction and analysis of the test results, a generalized porosity model considering the increase of the porosity and decrease of the effective bearing area of the mortar sample in the corrosion process was proposed. The relation between the uniaxial compressive strength and the corrosion time of the corroded mortar is deduced, and the unknown parameters are determined based on the regression analysis of the test data.

Data Availability

The data used to support the findings of this study are available from the corresponding author upon request.

Conflicts of Interest

The authors declare that they have no conflicts of interest.

Acknowledgments

The authors would like to thank the National Natural Science Foundation of China (41172237) for supporting this research project and also thank Guojie Wang and Fei Han for their contribution to this paper.

References

[1] ACI 515.2R-13, *Guide to Selecting Protective Treatments for Concrete ACI Committee 515*, American Concrete Institute, Farmington Hills, MI, USA, 2013.

[2] J. Zelić, R. Krstulović, E. Tkalćec, and P. Krolo, "Durability of the hydrated limestone-silica fume Portland cement mortars under sulphate attack," *Cement and Concrete Research*, vol. 29, no. 6, pp. 819–826, 1999.

[3] E. F. Irassar, V. L. Bonavetti, and M. Gonzalez, "Microstructural study of sulfate attack on ordinary and limestone Portland cements at ambient temperature," *Cement and Concrete Research*, vol. 33, no. 1, pp. 31–41, 2003.

[4] P. M. Carmona-Quiroga and M. T. Blanco-Varela, "Use of barium carbonate to inhibit sulfate attack in cements," *Cement and Concrete Research*, vol. 69, pp. 96–104, 2015.

[5] T. Kanazu, T. Matsumura, T. Nishiuchi, and T. Yamamoto, "Effect of simulated acid rain on deterioration of concrete," *Water, Air, and Soil Pollution*, vol. 130, no. 1–4, pp. 1481–1486, 2001.

[6] Z. G. Song, S. Y. Yang, Z. Liu, W. J. Mai, and H. Y. Li, "Material degradation of RC structures attacked by acid rain-a field investigation in Kunming," *Concrete*, vol. 217, no. 11, pp. 23–27, 2007.

[7] Y. Wang, D. T. Niu, and Z. P. Song, "Effect of acid rain erosion on steel fiber reinforced concrete," *Journal of Wuhan University of Technology-Mater. Sci. Ed.*, vol. 32, no. 1, pp. 121–128, 2017.

[8] Z. H. Wang, Z. M. Zhu, X. Sun, and X. M. Wang, "Deterioration of fracture toughness of concrete under acid rain environment," *Engineering Failure Analysis*, vol. 77, pp. 76–84, 2017.

[9] R. Chen, K. Yang, X. J. Qiu et al., "Degradation mechanism of CA mortar in CRTS I: slab ballastless railway track in the Southwest acid rain region of China-Materials analysis," *Construction and Building Materials*, vol. 149, pp. 921–933, 2017.

[10] K. Sobolev and A. Yeğinobali, "The development of high-strength mortars with improved thermal and acid resistance,," *Cement and Concrete Research*, vol. 35, no. 3, pp. 578–583, 2005.

[11] P. W. Brown and J. R. Clifton, "Mechanism of deterioration in cement-based materials and lime mortar," *Durability Building Materials*, vol. 5, pp. 409–420, 1988.

[12] R. Sersale, G. Frigione, and L. Bonavita, "Acid deposition and concrete attack: main influences," *Cement and Concrete Research*, vol. 28, no. 1, pp. 19–24, 1998.

[13] X. B. Hu, X. Y. Hou, X. M. Tao, F. Liu, and B. J. Xiao, "Analysis for composition change on acid rain attacking hydrated cement past," *Journal of Railway Science and Engineering*, vol. 4, no. 4, pp. 47–51, 2007.

[14] Y. F. Fan, Z. Q. Hu, Y. Z. Zhang, and J. L. Liu, "Deterioration of compressive property of concrete under simulated acid rain environment," *Construction and Building Materials*, vol. 24, no. 10, pp. 1975–1983, 2010.

[15] K. Yang, J. Liu, Z. L. Shi, and B. X. Li, "Research on the properties of mortar under strong acidic environment," *Concrete*, vol. 2, pp. 113–115, 2011.

[16] E. Franzoni and E. Sassoni, "Correlation between microstructural characteristics and weight loss of natural stones exposed to simulated acid rain," *Science of the Total Environment*, vol. 412-413, pp. 278–285, 2011.

[17] Z. G. Song and X. S. Zhang, "Experimental study of mortar under corrosion in sulfuric acid," *Journal of Building Materials*, vol. 15, no. 2, pp. 163–167, 2012.

[18] Y. F. Fan and H. Y. Luan, "Pore structure in concrete exposed to acid deposit," *Construction and Building Materials*, vol. 49, pp. 407–416, 2013.

[19] R. K. Huo, Q. Wang, B. Wang, H. W. Xin, and S. G. Li, "Acoustic properties variation analysis of the sandstone in acidic solution," *Journal of Xi'an University of Architecture and Technology (Natural Science Edition)*, vol. 48, no. 1, pp. 41–46, 2016.

[20] S. D. Xie, L. Qi, and D. Zhou, "Investigation of the effects of acid rain on the deterioration of cement concrete using accelerated tests established in the laboratory," *Atmospheric Environment*, vol. 38, no. 27, pp. 4457–4466, 2004.

[21] G. Y. Li, G. J. Xiong, Y. H. Lü, and Y. G. Yin, "The physical and chemical effects of long-term sulphuric acid exposure on hybrid modified cement mortar,," *Cement and Concrete Composites*, vol. 31, no. 5, pp. 325–330, 2009.

[22] Y. B. Wei, "Study on anti-acid corrosion performance of different types of cement mortar," *China Concrete and Cement Products*, vol. 12, pp. 62–65, 2012.

[23] M. C. Chen, K. Wang, and L. Xie, "Deterioration mechanism of cementitious materials under acid rain attack," *Engineering Failure Analysis*, vol. 27, pp. 272–285, 2013.

[24] H. Y. Gu, S. G. Cheng, Y. H. Yang, and H. Z. Chen, "Experimental study on impact from acid rain on the parameter of shear strength of landslide soil body," *Water Resources and Hydropower Engineering*, vol. 42, no. 10, pp. 36–39, 2011.

[25] Z. B. Wang, M. Zhang, J. J. Chen, and C. Y. Zhang, "Effects of acid rain on mechanical properties of the shale in the slip zone of Jiweishan landslide in Wulong of Chongqing," *Hydrogeology and Engineering Geology*, vol. 44, no. 3, pp. 113–118, 2017.

[26] The Chinese National Standard GB175-2007, *Common Portland Cement*Standards Press of China, Beijing, 2007, in Chinese.

[27] JGJ/T 98-2011, *Specification for Mix Proportion Design of Masonry Mortar*, China Architecture and Building, Press Beijing, China, 2011, in Chinese.

[28] The Chinese National Standard GB/T17671-1999, *Method of Testing Cements-Determination of Strength*Standards Press of China, Beijing, 1999, in Chinese.

[29] T. L. Han, J. P. Shi, Y. S. Chen, S. Dang, and P. Su, "Salt solution attack induced mechanical property degradation and quantitative analysis method for evolution of meso-structure damages of mortar," *Chinese Journal of Materials Research*, vol. 29, no. 12, pp. 921–930, 2015.

[30] X. H. Guo, B. L. Zhu, and H. N. Wu, "Corrosion mechanism of hydrochloric acid on concrete," *Concrete*, vol. 3, no. 4, pp. 8–10, 1991.

[31] X. H. Guo, "Discussion on durability of concrete under acid medium," *Concrete*, vol. 4, no. 1, pp. 35–38, 1992.

[32] U. Schneider and S. W. Chen, "The chemomechanical effect and the mechanochemical effect on high-performance concrete subjected to stress corrosion,," *Cement and Concrete Research*, vol. 28, no. 4, pp. 509–522, 1998.

[33] C. L. Bellego, B. Gerard, and G. Pijaudier, "Chemo-mechanical effect in mortar beams subjected to water hydrolysis," *Journal of Engineering Mechanics*, vol. 126, no. 3, pp. 266–272, 2000.